HHS Public Access

Author manuscript

Eur J Immunol. Author manuscript; available in PMC 2020 September 01.

Published in final edited form as:

Eur J Immunol. 2019 September ; 49(9): 1399–1414. doi:10.1002/eji.201847988.

MHC-restricted Ag85B-specific CD8+ T cells are enhanced by recombinant BCG prime and DNA boost immunization in mice

Shihoko Komine-Aizawa[1,*], **Jiansheng Jiang**[2], **Satoru Mizuno**[3,4], **Satoshi Hayakawa**[1], **Kazuhiro Matsuo**[3,4], **Lisa F. Boyd**[2], **David H. Margulies**[2], **Mitsuo Honda**[1]

[1]Division of Microbiology, Department of Pathology and Microbiology, Nihon University School of Medicine

[2]Molecular Biology Section, Laboratory of Immune System Biology, NIAID, National Institutes of Health

[3]Japan BCG Laboratory

[4]The Research Institute of Tuberculosis, Japan Anti-Tuberculosis Association

Abstract

Despite efforts to develop effective treatments and vaccines, *Mycobacterium tuberculosis* (*Mtb*), particularly pulmonary *Mtb*, continues to provide major health challenges worldwide. To improve immunization against the persistent health challenge of *Mtb* infection, we have studied the $CD8^+$ T cell response to Bacillus Calmette-Guérin (BCG) and recombinant BCG (rBCG) in mice. Here, we generated $CD8^+$ T cells with an rBCG-based vaccine encoding the Ag85B protein of *M. kansasii*, termed rBCG-Mkan85B, followed by boosting with plasmid DNA expressing the Ag85B gene (DNA-Mkan85B). We identified two MHC-I ($H2\text{-}K^d$)-restricted epitopes which induce cross-reactive responses to *Mtb* and other related mycobacteria in both BALB/c ($H2^d$) and CB6F1 ($H2^{b/d}$) mice. The $H2\text{-}K^d$-restricted peptide epitopes elicited polyfunctional $CD8^+$ T cell responses that were also highly cross-reactive with those of other proteins of the Ag85 complex. Tetramer staining indicated that the two $H2\text{-}K^d$-restricted epitopes elicit distinct $CD8^+$ T cell populations, a result explained by the X-ray structure of the two peptide/$H2\text{-}K^d$ complexes. These results suggest that rBCG-Mkan85B vector-based immunization and DNA-Mkan85B boost may enhance $CD8^+$ T cell response to *Mtb*, and might help to overcome the limited effectiveness of the current BCG in eliciting tuberculosis immunity.

Graphical Abstract

Ag85B specific polyfunctional $CD8^+$ T cells are inducible by recombinant BCG encoding the Ag85B protein of *Mycobacterium kansasii* (rBCG-Mkan85B), followed by boosting with plasmid

*Corresponding author: Shihoko Komine-Aizawa, 30-1 Oyaguchikamicho Itabashi-ku Tokyo Japan, aizawa.shihoko@nihon-u.ac.jp, Phone +81-3-3972-9560, FAX +81-3-3972-9560.

S.K.-A., J.J., M.H. and D.H.M. designed experiments; M.H. and K.M. constructed rBCG-Mkan85B and DNA-Mkan85B; S.K.-A. and M.H. performed immunization of animals and immunological analysis; L.F.B. and J.J. produced and purified MHC proteins; J.J. performed crystallization, data-collection, and X-ray structure determination; S.M., S.H. and K.M. provided technical assistance and scientific advice; S.K.-A., M.H. and D.H.M. wrote the manuscript.

Conflicts of Interest

The authors declare that they have no conflicts of interest or competing financial interests.

DNA expressing the Ag85B gene (DNA-Mkan85B). We identified two MHC-I (H2-K^d)-restricted epitopes which induce cross-reactive responses to *M. tuberculosis* and other mycobacteria.

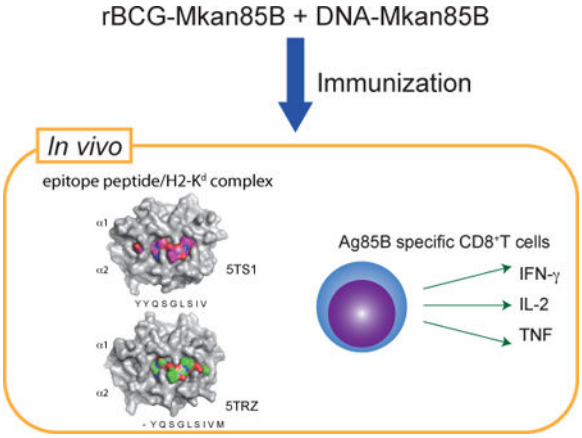

Keywords

MHC-I presentation; CD8$^+$ T Cells; CD4$^+$ T Cells; *Mycobacterium tuberculosis*; recombinant BCG

Introduction

The only available vaccine for *Mycobacterium tuberculosis* (*Mtb*) is a live attenuated strain of *Mycobacterium bovis*, termed Bacillus Calmette-Guérin (BCG), that induces pathogen-specific CD4$^+$ T cells which contribute to the protective immune response against subsequent *Mtb* infection by inducing inflammatory cytokines [1–3] and central memory CD4$^+$ T cells [4–6]. However, BCG has a limited ability to activate the CD8$^+$ T cell response for controlling the spread of tuberculosis (TB) [7, 8], while after infection with *Mtb*, CD8$^+$ T cells contribute to immunity by producing cytokines and acquire cytolytic function leading to lysis of infected cells and release of bacteria for extracellular killing [7, 9–12]. Although cross presentation of antigen is often crucial to the induction of pathogen-specific CD8$^+$ T cells, BCG antigens are relatively inefficiently presented by this MHC-I pathway [13].

Recombinant BCG (rBCG)-based vectors have been used in a variety of applications to induce CD8$^+$ T cell immunity [14] and other responses and have been more effective in eliciting *Mtb* resistance than BCG alone [15–19]. Several different rBCG vaccines and immunization strategies have been explored, including introduction of immunodominant *Mtb*-specific antigens that are lacking in BCG, such as the 6-kilodalton early-secreted antigenic target protein (ESAT-6), the mycobacterial protein from species TB (MPT64) [20–22]. Use of rBCG VPM1002 (BCGΔ*ure*C::hly) has demonstrated increased immunogenicity and efficacy by releasing BCG antigen and DNA into the cytosol of engulfed cells, then evoking autophagy, inflammasome activation and apoptosis of the cells [23–25]. Another approach is to modify BCG to improve mycobacterial antigen presentation by either infected cells or bystander cells [5, 26, 27]. Alternatively, over-expression of BCG antigens including

proteins of the Ag85 complex has been explored [17–19, 28–30]. Such rBCG for improving induction of mycobacteria-specific $CD4^+$ and $CD8^+$ T cells has been demonstrated [17].

The mycobacterial antigen 85 complex (Ag85) consists of three abundantly secreted proteins (Ag85A, Ag85B, and Ag85C). Ag85 proteins play an important role in mycobacterial pathogenesis and also exhibit cell wall mycolyltransferase activity[31], and may induce a strong T-cell proliferative response and IFN-γ production in healthy individuals exposed to *M. tuberculosis* and *M. leprae* [32, 33]. Therefore, Ag85 proteins have been used as mycobacterial antigens for new TB vaccines, such as recombinant BCG [17–19, 27, 34], DNA vaccines [35], subunit vaccines [36], and viral vector vaccines [37–39]. rBCG30 is the first constructed recombinant BCG overexpressing *Mtb* Ag85B in BCG. rBCG30 provided better protection from TB than BCG and has proven its safety in adults [17, 18]. These previous candidate vaccines studied by others have been based on *Mtb* Ag85B. We have been studying the BCG Ag85 complex, and the related Ag85 from *M. kansasii*, which causes a weak respiratory disease in immunocompromised humans. We previously noted that the protein sequence of *M. bovis* Ag85B (*Mbov*85B) was identical to that of *Mtb*85B [40], which is very similar to that of Ag85B of *M. kansasii* (*Mkan*85B) [41]. One approach is to clone and express these genes in vaccine vectors and to determine their effects in relation to the immune response to infection [40, 41]. In this study, we selected the Ag85B gene from *M. kansasii* (*Mkan*85B) which encodes a protein 89% identical to that of *Mtb*85B to generate a new rBCG (rBCG-Mkan85B) (Supporting Information Fig. S1) [41]. The rBCG-Mkan85B harboring the *Mkan*85B gene expresses the foreign protein at a high level in both mycobacterial cultures and upon infection of mammalian cells as described below. Moreover, we identified novel $CD8^+$ T cell epitopes of *Mtb*85B that induce polyfunctional $CD8^+$ T cells and that share functional epitopes with *Mkan*85B as well as *Mtb*85C and *Mtb*85A. We studied these epitopes structurally and functionally as well as their MHC restriction in a mouse model.

Results

BCG immunization fails to induce polyfunctional $CD8^+$ T cells specific for Mtb85B

Previous studies have shown that BCG immunization only weakly activates $CD8^+$ T cells in contrast to the robust activation of $CD4^+$ T cells [7, 8, 13]. We studied *Mtb*85B-specific polyfunctional $CD8^+$ and $CD4^+$ T cells after *in vivo* BCG priming followed by *in vitro* restimulation using PPD or pools of overlapping 15-mer peptides spanning the entire sequence of *Mtb*85B for restimulation. The gating strategy used to identify cytokines producing $CD8^+$ and $CD4^+$ T cells in spleen cells from mice is shown in Fig. 1A and the cells producing three, any two and any one cytokine were determined by Boolean combinations (Fig. 1A). Polyfunctional cells were counted as those making either two or more cytokines. No induction of $CD8^+$ T cells reactive with PPD or with peptide pools representing *Mtb*85B was observed following immunization with BCG in either $H2^d$ BALB/c (Fig. 1B) or $H2^b$ C57BL/6 mice (Fig. 1C). In contrast, BCG-induced polyfunctional $CD4^+$ T cells were detected following *in vitro* PPD stimulation in both $H2^b$ and $H2^d$ mice (Figs. 1B **and** C). Interestingly, peptide pool-5 of *Mtb*85B activated polyfunctional $CD4^+$ T cells only in $H2^b$ (Fig.1C), but not $H2^d$ mice (Fig.1B).

rBCG-Mkan85B/DNA-Mkan85B prime-boost immunization induce Mtb85B-specific polyfunctional CD8$^+$ T cells

To overcome the inability of BCG to induce an Ag85B specific CD8$^+$ T cell response, we increased the level of Ag85B antigen expression using a recombinant BCG that encodes *Mkan*85B in addition to the BCG-derived *Mbov*85B, designated rBCG-Mkan85B, and we revised the immunization procedure employing the prime boost regimen. We prepared rBCG-Mkan85B and plasmid DNA-Mkan85B (DNA-Mkan85B) as described in Materials and Methods. Western blot analysis of rBCG-Mkan85B lysates showed 9.3 times higher expression of an Ag85B protein than parental BCG lysates (Supporting Information Fig. S2A), while rBCG-Mbov85B expressed 1.8 times higher levels of Ag85B than parental BCG (Supporting Information Fig. S2A). To confirm that the Ag85B protein is expressible in mammalian cells as well, we transfected 293T cells with plasmid encoding Mkan85B named p3H-Mkan85B and analyzed this expression by SDS-PAGE and immunoblotting (Supporting Information Fig. S2B lane 4). Plasmid DNA-Mkan85B, used as a boosting DNA vaccine, which harbors the same *Mkan*85B gene, directed the expression of a protein, recognized by the Ag85B specific antibody, of the same size as that expressed by p3H-Mkan85B in 293T cells (Supporting Information Fig. S2B lane 2).

We immunized H2^d BALB/c and H2^b C57BL/6 mice by priming with rBCG-Mkan85B and boosting with plasmid DNA-Mkan85B (rBCG-Mkan85B/DNA-Mkan85B) (Supporting Information Fig. S3). We then quantified the *Mtb*85B specific polyfunctional CD8$^+$ and CD4$^+$ T cell responses in splenocytes from immunized mice using overlapping 15-mer peptides. In contrast to the failure to induce polyfunctional CD8$^+$ T cells following BCG immunization, rBCG-Mkan85B/DNA-Mkan85B elicited *Mtb*85B-specific polyfunctional CD8$^+$ T cells (Fig. 2). Stimulation was observed only with peptide pool-2 (Fig. 2A) and only in BALB/c mice, and was further localized to the H113 15-mer peptide (YYQSGLSIVMPVGGQ) (Fig. 2C). By contrast, CD8$^+$ T cells of C57BL/6 mice, despite being primed with rBCG-Mkan85B and boosted with plasmid DNA-Mkan85B, failed to respond to any *Mtb*85B peptide pools (Fig. 2B, D).

We then studied 9-mer peptides overlapping by eight amino acids, and identified two novel immunodominant CD8$^+$ T cell epitopes in *Mtb*85B -- Peptide-8 (pep8, YYQSGLSIV) and Peptide-9 (pep9, YQSGLSIVM) (Fig. 2E). These peptides stimulated responses similar to those of the parental 15-mer peptide (H113) at the same concentration (0.25μM) (Fig. 2C).

For the polyfunctional CD4$^+$ response to pool-5 in C57BL/6 mice, we identified the 15-mer peptide H149 (QDAYNAAGGHNAVFN) (Fig. 2D), a peptide that closely overlaps Peptide-25 (FQDAYNAAGGHNAVF), identified by others as one that induces a CD4$^+$ H2^b-restricted response [42–44]. However, as with BCG (Fig. 1), rBCG-Mkan85B immunization did not elicit polyfunctional *Mtb*Ag85B-specific CD4$^+$ T cells in BALB/c mice (Fig. 2A, C).

Differential stimulation of CD8$^+$ T cells with distinct peptide fine specificity

The amino acid sequences of the immunodominant CD8$^+$ T cell epitopes of pep8 (YYQSGLSIV) and pep9 (YQSGLSIVM) of *Mtb*85B are very similar to mycobacterial Ag85 complex proteins of other mycobacterial family members (Fig. 3A). rBCG-Mkan85B/

DNA-Mkan85B -immunization elicited responses that could be restimulated *in vitro* by peptides representing sequences from related Ag85 proteins from different mycobacterial species. As shown in Fig. 3A the pep8 epitope of *Mkan*85B (used in the vaccine) differs from pep8 of *Mtb*85B, *Mtb*85A, *Mbov*85A, and *Mle*85B. However, each pep8 variant elicited similar levels of polyfunctional T cells (Fig. 3B). For pep9, the substitution at residue 62 of D for Y in *Mtb*85A completely eliminated the *in vitro* response, while other versions of pep9 could elicit similar levels of polyfunctional $CD8^+$ T cells. Thus, the sharing of peptide sequences that induce polyfunctional $CD8^+$ T cell responses among proteins of the Ag85 complex in *Mtb* and other mycobacteria suggests that BCG85B-based immunization might be an effective to control mycobacterial infection.

Polyfunctional $CD8^+$ T cells specific for the pep8 and pep9 epitopes of Mtb85B in CB6F1 ($H2^{b/d}$) mice

We examined whether the potent generation of pep8- and pep9-specific $CD8^+$ T cells required $CD4^+$ T helper cells using F1 hybrid CB6F1 ($H2^{b/d}$) mice (Fig. 4A **and** 4B). On rBCG-Mkan85B/DNA-Mkan85B immunization, and *in vitro* restimulation with peptide, H149 induced polyfunctional $CD4^+$ T cells in both C57BL/6 and in CB6F1 animals. Whereas pep8 and pep9 induced only 0.4% and 0.3% polyfunctional $CD8^+$ cells in BALB/c, the response was augmented to 2.4% and 1.9% in CB6F1 respectively. Although pep8 and pep9 peptide stimulation was about six-fold more effective in CB6F1 than in BALB/c mice (Fig. 4A and 4B), there was no difference in the proportion of polyfunctional $CD4^+$ T cells in CB6F1 (0.7%) as compared with C57BL/6 (0.6%) as detected after H149 peptide stimulation (Fig. 4). Thus, immunization of $H2^{b/d}$ mice with rBCG-Mkan85B/DNA-Mkan85B improved the induction of pep8- or pep9-specific polyfunctional $CD8^+$ T cells, presumably due to the contribution of H149-specific $H2^b$-restricted $CD4^+$ helper T cells in CB6F1, suggesting that $CD4^+$ helper T cells contribute to the generation of potent $CD8^+$ effector T cells in the rBCG-Mkan85B-based prime boost immunization.

As rBCG-Mkan85B expressed 9.3 times higher levels of the Ag85B protein than parental BCG lysates, while rBCG-Mbov85B expressed 1.8 times higher levels of the Ag85B than parental BCG (Supporting Information Fig. S2A), we compared the immunogenicity of rBCG-Mkan85B with rBCG-Mbov85B. We immunized $H2^{b/d}$ CB6F1 mice by priming with rBCG-Mkan85B and boosting with plasmid DNA-Mkan85B (rBCG-Mkan85B/DNA-Mkan85B) or rBCG-Mbov85B and boosting with plasmid DNA-Mbov85B (rBCG-Mbov85B/DNA-Mbov85B). We studied polyfunctional $CD8^+$ T cells after immunization followed by *in vitro* restimulation with pep8 or pep9. rBCG-Mkan85B/DNA-Mkan85B enhanced the $CD8^+$ T cell response, while rBCG-Mbov85B/DNA-Mbov85B immunization did not induce pep8- or pep9-specific polyfunctional $CD8^+$ cells (Supporting Information Fig. S4).

Properties of the pep8- and pep9-specific polyfunctional $CD8^+$ T cells

Having shown that rBCG-Mkan85B/DNA-Mkan85B enhanced the $CD8^+$ T cell response in CB6F1 mice, we evaluated functional properties of the peptide-specific $CD8^+$ T cells. Dose-response analysis of pep8 and pep9 showed differences in the generation of polyfunctional $CD8^+$ T cells. Pep8 is more potent than pep9 for peptide-specific $CD8^+$ T cell induction--

pep9 produces half-maximal stimulation of polyfunctional T cells at a concentration of ~ 4.0 × 10^{-9} M, while even at 2.5 × 10^{-12} M pep8 achieves near maximal stimulation (Fig. 5A).

Furthermore, the level of surface expression of CD107a/b, an indicator of granule exocytosis, on peptide-specific $CD8^+$ T cells was significantly elevated to 85.8 ± 3.6% and 82.0 ± 6.1% by stimulation with pep8 and pep9, respectively (Fig. 5B, C). In contrast, polyfunctional $CD8^+$ T cells elicited by stimulation with PMA and ionomycin showed low surface expression of CD107a/b (Fig. 5B, C). These results indicate that the rBCG-based vectors can prime $CD8^+$ T cells to effectively induce peptide-specific effector $CD8^+$ T cells by $H2^d$-restricted epitopes of *Mtb*85B.

MHC class I specificity of Mtb85B-activated $CD8^+$ T cells

To identify the particular $H2^d$ MHC-I molecule(s) presenting pep8 or pep9 peptides to the immunization-elicited T cells, we used C1498 ($H2^b$) cell lines expressing transfected H2-K^d, H2-D^d, or H2-L^d as antigen presenting cells. *In vitro* re-stimulation of BALB/c splenocytes from animals immunized with rBCG-Mkan85B/DNA-Mkan85B, by pep9 peptide-pulsed C1498 cells, indicated that only the H2-K^d expressing transfectants stimulated the polyfunctional T cells (Fig. 6A).

To confirm the H2-K^d-restriction of the presentation of pep9 and to explore that of pep8 as well, we restimulated splenocytes from rBCG-Mkan85B/DNA-Mkan85B-immunized animals with peptide and blocked with specific mAb (Fig. 6B, C). In both BALB/c and CB6F1 animals, only mAb 34.1.2, which is specific for both H2-K^d and H2-D^d, inhibited the polyfunctional response, while mAbs 34.5.8 (anti-H2-D^d) and 30.5.7 (anti-H2-L^d) had no effect. Thus, both functional peptide epitopes, pep8 and pep9 of *Mtb*85B, are H2-K^d restricted.

We confirmed the specificity of the $CD8^+$ T cell responses elicited by the rBCG-Mkan85B/DNA-Mkan85B prime boost regimen with H2-K^d tetramers prepared with pep8 and pep9. K^d-pep8 and K^d-pep9 tetramers stained 0.9% and 0.2% of the $CD8^+$ T cells from spleens of BALB/c (Fig. 6 D, E). Consistent with the greater potency of pep8 as compared with pep9 in dose-response titrations (Fig. 5A), although both pep8 and pep9 elicit specific $CD8^+$ polyfunctional T cells, pep8 consistently gives a stronger response.

Since the rBCG-Mkan85B/DNA-Mkan85B-induced T cells were stained by both H2-K^d-pep8 and H2-K^d-pep9 tetramers, we wondered whether this was due to cross-reactivity of the same T cells on the two different epitopes, or whether these T cells expressed TCR of distinct reactivity. Double staining with the two tetramers labelled with different fluorochromes (Fig. 6F) revealed that most of the T cells (1.6%) stained only with the pep8/H2-K^d tetramer and a smaller population (0.12%) stained only with the pep9/H2-K^d tetramer, but very few (0.005%) stained simultaneously with both tetramers. Thus, although the rBCG-Mkan85B/DNA-Mkan85B elicits an H2-K^d-restricted response with two overlapping peptides, the bulk of the T cells are unique for one or the other epitope, and few cells react with both.

Structural analysis of pep8 and pep9 peptide/H2-K^d complexes

To gain mechanistic insight into the molecular basis of the H2-K^d-restricted T cell recognition of the *Mtb*Ag85B-derived epitopes, we determined the structures of the pep8/H2-K^d and pep9/H2-K^d complexes by X-ray crystallography (Table 1). The structures of the peptide/MHC-I/β_2m complexes for pep8 and pep9 (Fig. 7) were determined to 2.3 and 2.25 Å respectively, and satisfied standard validation criteria for protein structures determined at these resolutions. The complexes with pep8 or pep9 were remarkably similar with rmsd of 0.360 Å for superposed 336 Cα atoms. In addition, the backbone fold of each complex consistently superposed with rmsd of less than 1.0 Å for all other H2-K^d molecules in the protein database. Of particular note, however, is the disposition of the two nanomer peptides in their respective structures: pep8 is situated in the binding groove in a canonical conformation, consistent with previously published H2-K^d structures, with Y2 of the peptide buried in the B pocket of H2-K^d, and V9 in the F pocket (Fig. 7A, C, E, and G). However, pep9 is bound with its single Y1 in the B pocket, and the penultimate V8 in the F pocket, with the C-terminal M9 laying in a concavity formed in part by H2-K^d Y84, T80 and Y123 (Fig7B, D, F, **and** H). The C-terminal carboxylate of pep9 is exposed to solvent. The A pocket, which normally accommodates the amine of the N-terminal amino acid, is occupied by Y1 in the pep8 complex, but is occupied with several water molecules in the pep9 structure (Fig. 7G). Superposition of the bound peptides graphically illustrates this aspect of the comparison of the two structures -- backbone atoms as well as side chains of pep8 residues 2 through 9 superpose extremely closely with pep9 residues 1 through 8 (rmsd of 8 Cα atoms of 0.146 Å) (Fig. 7C, D). These structures reinforce the structural basis of the H2-K^d motif to be Y at position 2 and a short chain hydrophobic residue at position 9, and provide an understanding of how peptides with a single N-terminal Y may bind with the position 1 side chain in the B pocket. The striking difference in surface charge between the pep8 and pep9 complexes results from the flipping out of the C-terminus of pep9 due to the penultimate residue (V8 of pep9) being bound in the F pocket (Fig. 7I). This suggests that T cells bearing receptors that bind pep8/H2-K^d would not be expected to bind pep9/H2-K^d complexes.

Discussion

Different arms of the immune system play a role in resistance to TB, and so efforts to develop immunization strategies include approaches to stimulate both adaptive and innate immunity as well as to improve both CD8$^+$ and CD4$^+$ T cell responses. Here we have focused on an approach that, in the appropriate genetic background, enhances CD8$^+$ T cell responses to epitopes of a conserved region of Ag85 molecules. CD8$^+$ T cells possess multiple mechanisms to eliminate *Mtb* [7, 10, 45, 46]. Depletion or knockout of CD8$^+$ T cells significantly decreases immunological responses against tuberculosis and increases susceptibility to *Mtb* [47, 48]. Although BCG vaccination has been used to improve resistance to *Mtb*, it does not adequately control tuberculosis and new candidate vaccines have been explored to achieve more effective protection against infection [7, 15, 49–51]. BCG immunization induces a delayed and weak CD8$^+$ response when compared with *Mtb* infection [8, 13]. In this study, we observed that BCG immunization and *in vitro* restiulation with *Mtb*85B peptides could not induce polyfunctional CD8$^+$ T cells in either H2^b or H2^d

mice. We previously suggested that BCG could be useful in prime boost strategies to induce CD8 immunity to HIV envelope proteins [14, 52]. Here, we explored the use of BCG as a vector for directing the expression of mycobacterial proteins that might similarly elicit CD8 responses, and studied the proteins of the Ag85 complex, in particular, *Mkan*85B. The Ag85B protein is one member of the Ag85 complex consisting of Ag85A, Ag85B and Ag85C, which are major secreted products of mycobacteria and have been investigated as candidates for induction of protective immunity [7, 16, 18, 31, 38, 40, 53]. All three Ag85 proteins are highly conserved among mycobacterial species [31, 38, 54]. We observed that a recombinant BCG expressing *Mkan*85B (rBCG-Mkan85B) produced more Ag85B than the endogenous *Mbov*85B, and that immunization with rBCG-Mkan85B, followed by boosting with a plasmid encoding the *Mkan*85B could elicit CD8 T cells that responded to *Mtb*85B peptides. This CD8 response was only observed in BALB/c ($H2^d$) and not in C57BL/6 ($H2^b$) mice, although a CD4 response was readily detected in C57BL/6 ($H2^b$). Thus, the presentation of $CD8^+$ and $CD4^+$ epitopes from *Mtb*85B was dependent on $H2^d$ or $H2^b$ respectively.

Mapping of the antigenic epitopes of *Mtb*85B in BALB/c ($H2^d$) animals identified two peptides, pep8 and pep9 as the YYQSGLSIV and YQSGLSIVM sequences (amino acids 61–69 and 62–70, respectively). Both epitopes were presented by the H2-K^d, as demonstrated with transfected APC and with specific monoclonal antibody blocking. The previous failure to identify these epitopes might be due to the difference of the expressed proteins, i.e. our *Mkan*85B single protein as compared to a single fusion protein composed of *Mtb*85A, *Mtb*85B and TB10.4 [38]. In processing of the fusion protein, immunodominant CD8 epitopes on Ag85B might be masked and another MHC-I epitope might become immunodominant [38]. Alternatively, it may depend on the different type of priming antigens, i.e. our rBCG-Mkan85B vector-based prime boost regimen in contrast with proteins, plasmid DNA or adenovirus vector [38, 44, 55]; or that rBCG infects antigen presenting cells and resides primarily in vacuoles. When the rBCG is degraded, the escape into the cytoplasm may lead to expression of Ag85B in the mammalian cells. In contrast, adenovirus and plasmid DNA vectors may direct the expression of foreign *Mtb* antigens to different antigen presentation pathways. Another possible explanation is the difference in length of peptides used for the mapping of $CD8^+$ T cells [44, 55, 56].

The CD4 response in C57BL/6 ($H2^b$) was due to a 15-mer peptide, presumably IA^b restricted, that was almost identical to one previously identified as Peptide-25 by others [42, 43]. On the other hand, we did not detect $CD4^+$ T cell epitopes of Ag85B recognized by BALB/c mice ($H2^d$) in agreement with previous reports [38, 44, 55].

The simplest interpretation of these studies suggested that F1 animals capable of presenting both the MHC-I (H2-K^d) and MHC-II (IA^b) –restricted epitopes would mount the best response. This was confirmed by evaluating the proportion of polyfunctional $CD8^+$ and $CD4^+$ T cells in either the BALB/c or C57BL/6 parental strains or the CB6F1 hybrid ($H2^{b/d}$). Interestingly, the magnitude of the $CD8^+$ response in the CB6F1 mice was six-fold higher when compared with that in BALB/c mice. These observations suggest that the generation of a potent *Mtb*85B-specific polyfunctional $CD8^+$ T cell response is improved by the simultaneous elicitation of an *Mtb*85B-specific CD4 response in these animals.

To understand further the nature of the CD8 response, which resulted from priming and boosting with *Mkan*85B and was then detected *in vitro* with the homologous *Mtb*85B-derived peptides, pep8 and pep9 were compared quantitatively, and recall responses with related *Mtb*85A, *Mkan*85B, and *Mle*85B were examined. These studies provided initial information on the relative potency of pep8 and pep9, and also revealed sequence dependency of the stimulation by different related but distinct peptides. That the two overlapping peptides, pep8 and pep9, showed different quantitative effects prompted us to explore the relationship of the T cells elicited by the immunization strategy. Staining with specific peptide/H2-K^d tetramers indicated that most of these T cells were specific for pep8/H2-K^d complexes, that some revealed specificity for pep9/H2-K^d, and that few reacted with both peptide/H2-K^d reagents. Thus, the $CD8^+$ T cell populations, which are induced by rBCG-Mkan85B/DNA-Mkan85B prime boost immunization, are unique for one or the other epitope.

The X-ray crystal structures of the two peptide/H2-K^d complexes revealed striking differences not only in the mode of peptide binding, but also in the apparent surface charge of the complexes due to distinct orientation of the peptides in the pep8 as compared with the pep9 complex. Pep8 (YYQSGLSIV) binds H2-K^d in the canonical configuration observed for several different nonamer peptide/H2-K^d complexes [57–61]. That is, the P2 residue, Y, is anchored tightly in the B pocket of H2-K^d and the C-terminal residue, V, is firmly planted in the F pocket. All other H2-K^d structures in the protein database show P2 Y or F in the B pocket, and all but the decamer with G9GF (LYLVCGERGF) [60] locate the C-terminal residue to the F pocket. The pep9 (YQSGLSIVM) structure reported here explains how peptides that have P1 Y can plant that side chain into the B pocket, leaving the A pocket occupied by water molecules. Pep9, like the G9GF peptide, is bound with the C-terminal residue side chain lying flat in an auxiliary “G” pocket, that lies distal to the canonical F pocket, generated by the lateral rotation of H2-K^d residue Y84. This forces the C-terminal carboxylate to be exposed to solvent, changing the peptide-dependent electrostatic charge, and altering the requirement for TCR interaction. These conformational differences between the pep8/H2-K^d and pep9/H2-K^d complexes explain the distinct recognition by different T cell populations.

The rBCG-Mkan85B/DNA-Mkan85B prime boost scheme not only induced polyfunctional (i.e. double and triple positive IFN-**γ**, IL-2 and TNF- producing cells), as analyzed cytometrically, it also increased, in an epitope-specific response, the expression of CD107a/b, an indicator of granule exocytosis, on the CD8 T cells. This contrasts with the non-specific stimulation by PMA-ionomycin that failed to induce CD107 expression, and emphasizes the value of the immunization scheme in directing an additional immunologically relevant effector function.

Several recombinant BCG strains have been developed as novel TB vaccine by others. rBCG30, which overexpresses *Mtb* Ag85B, provided better protection from TB than parental BCG and has proven its safety in adults [17, 18]. VPM1002, in which the *ureC* of BCG has been replaced by the listeriolysin O (LLO) encoding gene (*hly*) from *Listeria monocytogenes* is one of the most advanced recombinant BCG. The expression of LLO in VPM1002 causes bacterial products to escape to the cytosol, then the bacterial antigens are

presented by MHC-class I pathway. VPM1002 provided better efficacy than BCG due to induction of specific CD4 and CD8 T cell response [23–25]. In this study, we showed rBCG-Mkan85B produced more Ag85 protein than parental BCG or rBCG-Mbov85B. rBCG-Mkan85B/DNA-Mkan85B immunization could elicit *Mtb*85B-specific polyfunctional $CD8^+$ T cells besides $CD4^+$ T cells. We also found two H2-K^d-restricted peptide epitopes that elicited polyfunctional $CD8^+$ T cell responses that were also highly cross-reactive with those of other proteins of the Ag85 complex. The structures of H2-K^d complexes with each of these epitope peptides were determined by X-ray crystallography. Our data further suggest that understanding the mechanism of immature $CD8^+$ T cell activation by BCG immunization in mouse model systems may contribute to approaches to improve BCG vaccine efficacy against *Mtb* and to the rational design of a TB vaccine. Thus, modifications of BCG as addressed in our study may prove to be effective in enhanced activation of $CD8^+$ T cells resulting in more efficient control of *Mtb* infection.

Materials and Methods

Animals

Specific pathogen-free female mice; BALB/c ($H2^d$), C57BL/6 ($H2^b$) and CB6F1 mice were purchased from Japan SLC Inc., Shizuoka, Japan and CLEA Japan, Inc., Tokyo. All animal studies were carried out in Japan under institutional guidelines approved by Nihon University Animal Care and Use Committee and The Research Institute of Tuberculosis, Japan Anti-Tuberculosis Association Animal Care and Use Committee, and the institutional committee for gene-recombination experiemtns and bio-risk management and control. Institutional animal experimental guidelines are in accordance with ILAR Guide. Mice were allowed free access to sterile water and standard mouse food, and physiological conditions were assessed every few days.

Shuttle vector, generation of rBCG-Mkan85B, plasmid DNA-Mkan85B

Freeze-dried BCG vaccine was rehydrated in cold sterile water. We prepared rBCG vectors expressing the *Mkan*85B gene [41] or *Mbov*85B gene [40] modifying previous procedures with the *E. coli-mycobacteria* plasmids p3H8.4 containing mycobacterium promoter from Dr. G.J. Nabel [14, 52, 62]. Plasmid DNA expressing the Ag85B gene (DNA-Mkan85B) was prepared as booster antigen. For preparation of shuttle plasmid and rBCG-Mkan85B-expressing Ag85B gene, we employed two kinds of vectors. One is a previously characterized p3H8.4 vector [52] composed of the *pAL5000* gene from pSO246 [14] and CMV enhancer/promoter from VRC8400. The other, a pKAH20 vector [41] encoding the gene of *Mkan85B*, which was subcloned as an *XbaI*/BamHI fragment into p3H8.4 (p3H-Mkan85B). We also used pαL-1 vector for preparation of p3H-Mbov85B [40]. p3H-Mkan85B or p3H-Mbov85B were electroporated into cultured BCG using Gene Pulser (Bio-Rad). rBCG-Mkan85B and rBCG-Mbov85B were cloned and a single colony was passaged once on a Middlebrook 7H10 agar (Difco) plate supplemented with oleic acid albumin dextrose complex (OADC) enrichment (Difco) containing kanamycin. Plasmid DNA-Mkan85B encoding the *Mkan*85B gene was prepared by inserting the DNA fragment encoding the *Mkan85B* gene into the existing *Xba*I/*Bam*HI sites in VRC8400 [52].

Expressions of *Mkan*85B or *Mbov*85B protein in rBCG lysate and plasmid DNA-Mkan85B-transfected 293T cells are described in the legend to Figure S2.

Immunization

Mice were immunized with BCG vaccine or rBCG-Mkan85B at a concentration of 4×10^6 CFU or 0.1 mg of bacilli i.d., and 100 μg of plasmid DNA or control DNA in saline i.m. three times [52] (Supporting Information Fig. S3).

Polychromatic flow cytometry for intracellular cytokine production and detection of tetramer positive cells

Peptides covering the whole *Mtb*85B protein, synthesized as 15-mers with a 10 amino acid overlap, were first used to identify pools that stimulated $CD8^+$ and $CD4^+$ T cells. Then, individual 15-mers were analyzed, and subsequently 9-mers overlapping by 8 amino acids were examined to determine the minimal $CD8^+$ T cell epitopes. Tuberculin PPD (PPD) was kindly supplied by the Japan BCG Laboratory. Spleen cells were stimulated with peptides or PPD (2 μg/ml) and stained for cell surface or intracellular cytokines IFN-γ, IL-2, and TNF, as described previously [52, 63]. A seven-colour flow cytometry panel was used to simultaneously analyse multiple cytokines at the single-cell level. The gating strategy used to identify cytokines producing $CD8^+$ and $CD4^+$ T cells in spleen cells from mice is shown in Fig. 1A. Following *in vitro* stimulation for 6 hours, cells were incubated with ViViD dye to identify dead cells followed by surface staining with antibodies against CD3-V500 (BD) or CD3-APC, CD8-PerCp-Cy5.5 (BioLegend) and CD4-PE-Cy7 (BD). Cells were then fixed and permeabilized using BD Cytofix/Cytoperm (BD) and stained for IFN-γ-PE, IL-2-APC-Cy7 and TNF-Alexa Fluor488 or TNF-APC (BioLegend) [2]. Since an individual responding cell could be present in more than one of the cytokine gates, the total response for any cytokine is less than the sum of all three gates. Thus, we used Boolean combinations of the three gates to uniquely discriminate responding cells based on their quality or functionality with respect to cytokine production. (Fig. 1A). Polyfunctional cells were counted as those making either two or more cytokines. Optimal concentrations of all antibodies including anti-CD107a-Alexa Fluor488 and anti-CD107b-Alexa Fluor488 (BioLegend) [64], used in this study were determined in pilot titration experiments.

For tetramer assay, splenocytes were incubated with PE- and/or APC-conjugated pep8/H2-K^d and pep9/H2-K^d tetramers containing human β_2m for 30 min at room temperature and then were stained for CD3-V500 (BD), CD8-PerCp-Cy5.5 (BioLegend), CD4-PE-Cy7 (BD), CD16/32 -Brilliant Violet 421(BioLegend), and CD19-Pacific Blue (eBiosciense) [52].

FACS analysis was performed using a FACSVerse (BD) or FACSCanto (BD) with FlowJo (Treestar) [2, 52].

We have adhered to the “Guidelines for the use of flow cytometry and cell sorting in immunological studies” for data analysis [65].

Analysis of the usage of H2 complex

For ICS, splenocytes were re-stimulated with epitope peptide-pulsed stimulator cells C1498 H2-D^d, C1498 H2-K^d, C1498 H2-L^d or C1498 cells (ATCC TIB-49) [66] which had been treated with mitomycin C (Sigma-Aldrich) for 1hr before re-stimulation. Then, polyfunctional $CD8^+$ T cells were analyzed for H2 expression. For blocking of the H2 complex-mediated pathway, cells were preincubated with antibodies specific for H2-D^d (mAb 34.5.8), H2-K^dD^d (mAb 34.1.2) or H2-L^d (mAb 30.5.7) [67] for 30 min on ice before ICS.

Protein expression, purification, crystallization, X-ray data collection, and crystallographic refinement

The luminal domain of H2-K^d cDNA (the gift of Dr. M. Zauderer) was expressed in pET3a in *E. coli* BL21, inclusion bodies were harvested, solubilized, and refolded with human β_2-microglobulin ($h\beta_2m$) and either peptide pep8 (YYSGLSIV) or pep9 (YSGLSIVM) by standard protocols [68, 69]. Peptide/H2-K^d complexes were purified by size exclusion chromatography on Superdex 75 and mono Q (GE Healthcare), and crystals were obtained in 14% PEG 4000, 0.1 M MES pH 6.5 containing 5% MPD. Data on individual crystals were collected remotely at Argonne Photon Source (SER-CAT beamline 22IDD), processed with XDS [70], and molecular replacement solutions identified with Phaser [71] using PDB 2Z76 with the peptide omitted as a probe. Refinement was accomplished with Phenix [72] and graphics illustration was accomplished with PyMOL (The PyMOL Molecular Graphics System, Version 1.7 Schrödinger, LLC). The complex with pep8, in the P1 space group with four molecules in the asymmetric unit (AU), refined to a resolution of 2.30 Å with a twin fraction of 0.45 (twin law, -h, k, -l) and R_{work}/R_{free} (%) of 18.7/22.5. The complex with pep9 was in $P2_1$, with two molecules in the AU, and refined to a resolution of 2.25 Å with a twin fraction of 0.48 (twin law, h, -k, -l) and R_{work}/R_{free} (%) of 19.3/21.6. Data collection and refinement statistics are given in Table 1. Since there were minimal differences among the different molecules in the AU, all discussion will be focused on the first peptide/H2-K^d/$h\beta_{2m}$ complex for either pep8 or pep9.

Data analysis and statistics

All comparisons between recombinant and control groups and between immunization groups were conducted using one-way ANOVA tests assuming variances with the JMP program (SAS Institute). Data are expressed as mean ± SEM.

Supplementary Material

Refer to Web version on PubMed Central for supplementary material.

Acknowledgements

The authors thank Dr. S. Yamamoto, Japan BCG Laboratory and Dr. K. Natarajan, NIAID, NIH for their helpful discussions and comments on the manuscript; Dr. K. Takada, Nihon University School of Medicine for support with protein analysis; Dr. N. Doi, The Research Institute of Tuberculosis, Japan Anti-Tuberculosis Association for helpful guidance for animal biosafety experiments; and Dr. G. J. Nabel, Vaccine Research Center, NIAID, NIH for providing the plasmids for the vaccine. We also thank the National Institute of Allergy and Infectious Diseases MHC Tetramer Core Facility for preparation of MHC-I/peptide tetramers. This work was funded by JSPS

KAKENHI Grant numbers JP16K09946 (for S.K.-A) and JP17K10035 (for M.H), MEXT-Surpprted Program for the Strategic Research Foundation at Private Universities “International joint research and training of young researchers for zoonosis control in the globalized world” (for S.K.-A), Nihon University Multidisciplinary Research Grant for 2016 (for S.K.-A). This work was supported in part by the intramural research program of the NIAID, NIH. Data were collected at Southeast Regional Collaborative Access Team (SER-CAT) 22-ID (or 22-BM) beamline at the Advanced Photon Source, Argonne National Laboratory. Supporting institutions may be found at www.ser-cat.org/members.html.Use of the Advanced Photon Source was supported by the U.S. Department of Energy, Office of Science, Office of Basic Energy Sciences, under Contract No. W-31–109-Eng-38. GM/CA@APS has been funded in whole or in part with Federal funds from the National Cancer Institute (ACB-12002) and the National Institute of General Medical Sciences (AGM-12006). This research used resources of the Advanced Photon Source, a U.S. Department of Energy (DOE) Office of Science User Facility operated for the DOE Office of Science by Argonne National Laboratory under Contract No. DE-AC02–06CH11357. The Eiger 16M detector was funded by an NIH–Office of Research Infrastructure Programs, High-End Instrumentation Grant (1S10OD012289–01A1).

Abbreviations used in this paper:

Mtb	*Mycobacterium tuberculosis*
TB	tuberculosis
BCG	*Mycobacterium bovis* bacillus Calmette-Guérin
rBCG	recombinant BCG
ICS	intra-cellular cytokine staining
Ag85	antigen 85 complex
Ag85A	antigen 85A
Ag85B	antigen 85B
Ag85C	antigen 85C
***Mtb*85B**	*Mycobacterium tuberculosis* antigen 85B
***Mtb*85C**	*Mtb* antigen 85C
***Mtb*85A**	*Mtb* antigen 85A
***Mbov*85B**	*Mycobacterium bovis* BCG antigen 85B
***Mbov*85C**	*Mbov* antigen 85C
***Mbov*85A**	*Mbov* antigen 85A
***Mkan*85B**	*M. kansasii* Ag85B
***Mav*85B**	*M. avium* Ag85B
***Min*85B**	*M. intracellulare* Ag85B
***Map*85B**	*M. avium subsp. paratuberculosis* Ag85B
***Mul*85B**	*M. ulcerans* Ag85B
***Mle*85B**	*M. leprae* Ag85B

CFU colony forming unit

Reference list

1. Kipnis A, Irwin S, Izzo AA, Basaraba RJ and Orme IM, Memory T lymphocytes generated by Mycobacterium bovis BCG vaccination reside within a CD4 CD44lo CD62 ligand(hi) population. Infect Immun 2005 73: 7759–7764. [PubMed: 16239580]
2. Darrah PA, Patel DT, De Luca PM, Lindsay RW, Davey DF, Flynn BJ, Hoff ST, Andersen P, Reed SG, Morris SL, Roederer M and Seder RA, Multifunctional TH1 cells define a correlate of vaccine-mediated protection against Leishmania major. Nat Med 2007 13: 843–850. [PubMed: 17558415]
3. Seder RA, Darrah PA and Roederer M, T-cell quality in memory and protection: implications for vaccine design. Nat Rev Immunol 2008 8: 247–258. [PubMed: 18323851]
4. Andersen P and Smedegaard B, CD4(+) T-cell subsets that mediate immunological memory to Mycobacterium tuberculosis infection in mice. Infect Immun 2000 68: 621–629. [PubMed: 10639425]
5. Vogelzang A, Perdomo C, Zedler U, Kuhlmann S, Hurwitz R, Gengenbacher M and Kaufmann SH, Central memory CD4+ T cells are responsible for the recombinant Bacillus Calmette-Guerin DeltaureC::hly vaccine's superior protection against tuberculosis. J Infect Dis 2014 210: 1928–1937. [PubMed: 24943726]
6. Soares AP, Kwong Chung CK, Choice T, Hughes EJ, Jacobs G, van Rensburg EJ, Khomba G, de Kock M, Lerumo L, Makhethe L, Maneli MH, Pienaar B, Smit E, Tena-Coki NG, van Wyk L, Boom WH, Kaplan G, Scriba TJ and Hanekom WA, Longitudinal changes in CD4(+) T-cell memory responses induced by BCG vaccination of newborns. J Infect Dis 2013 207: 1084–1094. [PubMed: 23293360]
7. Ottenhoff TH and Kaufmann SH, Vaccines against tuberculosis: where are we and where do we need to go? PLoS Pathog 2012 8: e1002607.
8. Ryan AA, Nambiar JK, Wozniak TM, Roediger B, Shklovskaya E, Britton WJ, Fazekas de St Groth B and Triccas JA, Antigen load governs the differential priming of CD8 T cells in response to the bacille Calmette Guerin vaccine or Mycobacterium tuberculosis infection. J Immunol 2009 182: 7172–7177. [PubMed: 19454714]
9. Cooper AM and Khader SA, The role of cytokines in the initiation, expansion, and control of cellular immunity to tuberculosis. Immunol Rev 2008 226: 191–204. [PubMed: 19161425]
10. Nunes-Alves C, Booty MG, Carpenter SM, Jayaraman P, Rothchild AC and Behar SM, In search of a new paradigm for protective immunity to TB. Nat Rev Microbiol 2014 12: 289–299. [PubMed: 24590243]
11. Mogues T, Goodrich ME, Ryan L, LaCourse R and North RJ, The relative importance of T cell subsets in immunity and immunopathology of airborne Mycobacterium tuberculosis infection in mice. J Exp Med 2001 193: 271–280. [PubMed: 11157048]
12. van Pinxteren LA, Cassidy JP, Smedegaard BH, Agger EM and Andersen P, Control of latent Mycobacterium tuberculosis infection is dependent on CD8 T cells. Eur J Immunol 2000 30: 3689–3698. [PubMed: 11169412]
13. Mazzaccaro RJ, Gedde M, Jensen ER, van Santen HM, Ploegh HL, Rock KL and Bloom BR, Major histocompatibility class I presentation of soluble antigen facilitated by Mycobacterium tuberculosis infection. Proc Natl Acad Sci U S A 1996 93: 11786–11791. [PubMed: 8876215]
14. Honda M, Matsuo K, Nakasone T, Okamoto Y, Yoshizaki H, Kitamura K, Sugiura W, Watanabe K, Fukushima Y, Haga S, Katsura Y, Tasaka H, Komuro K, Yamada T, Asano T, Yamazaki A and Yamazaki S, Protective immune responses induced by secretion of a chimeric soluble protein from a recombinant Mycobacterium bovis bacillus Calmette-Guerin vector candidate vaccine for human immunodeficiency virus type 1 in small animals. Proc Natl Acad Sci U S A 1995 92: 10693–10697. [PubMed: 7479867]
15. Skeiky YA and Sadoff JC, Advances in tuberculosis vaccine strategies. Nat Rev Microbiol 2006 4: 469–476. [PubMed: 16710326]
16. Kaufmann SH and Gengenbacher M, Recombinant live vaccine candidates against tuberculosis. Curr Opin Biotechnol 2012 23: 900–907. [PubMed: 22483201]

17. Hoft DF, Blazevic A, Abate G, Hanekom WA, Kaplan G, Soler JH, Weichold F, Geiter L, Sadoff JC and Horwitz MA, A new recombinant bacille Calmette-Guerin vaccine safely induces significantly enhanced tuberculosis-specific immunity in human volunteers. J Infect Dis 2008 198: 1491–1501. [PubMed: 18808333]

18. Horwitz MA and Harth G, A new vaccine against tuberculosis affords greater survival after challenge than the current vaccine in the guinea pig model of pulmonary tuberculosis. Infect Immun 2003 71: 1672–1679. [PubMed: 12654780]

19. Horwitz MA, Harth G, Dillon BJ and Maslesa-Galic S, Recombinant bacillus calmette-guerin (BCG) vaccines expressing the Mycobacterium tuberculosis 30-kDa major secretory protein induce greater protective immunity against tuberculosis than conventional BCG vaccines in a highly susceptible animal model. Proc Natl Acad Sci U S A 2000 97: 13853–13858. [PubMed: 11095745]

20. Dai FY, Wang JF, Gong XL and Bao L, Immunogenicity and protective efficacy of recombinant Bacille Calmette-Guerin strains expressing mycobacterium antigens Ag85A, CFP10, ESAT-6, GM-CSF and IL-12p70. Hum Vaccin Immunother 2017 13: 1–8.

21. Wang LM, Shi CH, Fan XL, Xue Y, Bai YL and Xu ZK, Expression and immunogenicity of recombinant Mycobacterium bovis Bacillus Calmette-Guerin strains secreting the antigen ESAT-6 from Mycobacterium tuberculosis in mice. Chin Med J (Engl) 2007 120: 1220–1225. [PubMed: 17697571]

22. Qie YQ, Wang JL, Liu W, Shen H, Chen JZ, Zhu BD, Xu Y, Zhang XL and Wang HH, More vaccine efficacy studies on the recombinant Bacille Calmette-Guerin co-expressing Ag85B, Mpt64 and Mtb8.4. Scand J Immunol 2009 69: 342–350. [PubMed: 19284499]

23. Kaufmann SH, Cotton MF, Eisele B, Gengenbacher M, Grode L, Hesseling AC and Walzl G, The BCG replacement vaccine VPM1002: from drawing board to clinical trial. Expert Rev Vaccines 2014 13: 619–630. [PubMed: 24702486]

24. Grode L, Ganoza CA, Brohm C, Weiner J 3rd, Eisele B and Kaufmann SH, Safety and immunogenicity of the recombinant BCG vaccine VPM1002 in a phase 1 open-label randomized clinical trial. Vaccine 2013 31: 1340–1348. [PubMed: 23290835]

25. Loxton AG, Knaul JK, Grode L, Gutschmidt A, Meller C, Eisele B, Johnstone H, van der Spuy G, Maertzdorf J, Kaufmann SH, Hesseling AC, Walzl G, Cotton MF and Group VPMS, Safety and Immunogenicity of the Recombinant Mycobacterium bovis BCG Vaccine VPM1002 in HIV-Unexposed Newborn Infants in South Africa. Clin Vaccine Immunol 2017 24.

26. Grode L, Seiler P, Baumann S, Hess J, Brinkmann V, Nasser Eddine A, Mann P, Goosmann C, Bandermann S, Smith D, Bancroft GJ, Reyrat JM, van Soolingen D, Raupach B and Kaufmann SH, Increased vaccine efficacy against tuberculosis of recombinant Mycobacterium bovis bacille Calmette-Guerin mutants that secrete listeriolysin. J Clin Invest 2005 115: 2472–2479. [PubMed: 16110326]

27. Sun R, Skeiky YA, Izzo A, Dheenadhayalan V, Imam Z, Penn E, Stagliano K, Haddock S, Mueller S, Fulkerson J, Scanga C, Grover A, Derrick SC, Morris S, Hone DM, Horwitz MA, Kaufmann SH and Sadoff JC, Novel recombinant BCG expressing perfringolysin O and the over-expression of key immunodominant antigens; pre-clinical characterization, safety and protection against challenge with Mycobacterium tuberculosis. Vaccine 2009 27: 4412–4423. [PubMed: 19500523]

28. Liu W, Xu Y, Shen H, Yan J, Yang E and Wang H, Recombinant Bacille Calmette-Guerin coexpressing Ag85B-IFN-gamma enhances the cell-mediated immunity in C57BL/6 mice. Exp Ther Med 2017 13: 2339–2347. [PubMed: 28565847]

29. Tang C, Yamada H, Shibata K, Maeda N, Yoshida S, Wajjwalku W, Ohara N, Yamada T, Kinoshita T and Yoshikai Y, Efficacy of recombinant bacille Calmette-Guerin vaccine secreting interleukin-15/antigen 85B fusion protein in providing protection against Mycobacterium tuberculosis. J Infect Dis 2008 197: 1263–1274. [PubMed: 18422438]

30. Liang J, Teng X, Yuan X, Zhang Y, Shi C, Yue T, Zhou L, Li J and Fan X, Enhanced and durable protective immune responses induced by a cocktail of recombinant BCG strains expressing antigens of multistage of Mycobacterium tuberculosis. Mol Immunol 2015 66: 392–401. [PubMed: 25974877]

31. Wiker HG and Harboe M, The antigen 85 complex: a major secretion product of Mycobacterium tuberculosis. Microbiol Rev 1992 56: 648–661. [PubMed: 1480113]

32. Launois P, DeLeys R, Niang MN, Drowart A, Andrien M, Dierckx P, Cartel JL, Sarthou JL, Van Vooren JP and Huygen K, T-cell-epitope mapping of the major secreted mycobacterial antigen Ag85A in tuberculosis and leprosy. Infect Immun 1994 62: 3679–3687. [PubMed: 7520418]
33. Launois P, Drowart A, Bourreau E, Couppie P, Farber CM, Van Vooren JP and Huygen K, T cell reactivity against mycolyl transferase antigen 85 of M. tuberculosis in HIV-TB coinfected subjects and in AIDS patients suffering from tuberculosis and nontuberculous mycobacterial infections. Clin Dev Immunol 2011 2011.
34. Lu Y, Xu Y, Yang E, Wang C, Wang H and Shen H, Novel recombinant BCG coexpressing Ag85B, ESAT-6 and Rv2608 elicits significantly enhanced cellular immune and antibody responses in C57BL/6 mice. Scand J Immunol 2012 76: 271–277. [PubMed: 22671973]
35. Hu D, Wu J, Zhang R and Chen L, T-bet acts as a powerful adjuvant in Ag85B DNAbased vaccination against tuberculosis. Mol Med Rep 2012 6: 139–144. [PubMed: 22552442]
36. Weinrich Olsen A, van Pinxteren LA, Meng Okkels L, Birk Rasmussen P and Andersen P, Protection of mice with a tuberculosis subunit vaccine based on a fusion protein of antigen 85b and esat-6. Infect Immun 2001 69: 2773–2778. [PubMed: 11292688]
37. McShane H, Pathan AA, Sander CR, Keating SM, Gilbert SC, Huygen K, Fletcher HA and Hill AV, Recombinant modified vaccinia virus Ankara expressing antigen 85A boosts BCG-primed and naturally acquired antimycobacterial immunity in humans. Nat Med 2004 10: 1240–1244. [PubMed: 15502839]
38. Radosevic K, Wieland CW, Rodriguez A, Weverling GJ, Mintardjo R, Gillissen G, Vogels R, Skeiky YA, Hone DM, Sadoff JC, van der Poll T, Havenga M and Goudsmit J, Protective immune responses to a recombinant adenovirus type 35 tuberculosis vaccine in two mouse strains: CD4 and CD8 T-cell epitope mapping and role of gamma interferon. Infect Immun 2007 75: 4105–4115. [PubMed: 17526747]
39. Watanabe K, Matsubara A, Kawano M, Mizuno S, Okamura T, Tsujimura Y, Inada H, Nosaka T, Matsuo K and Yasutomi Y, Recombinant Ag85B vaccine by taking advantage of characteristics of human parainfluenza type 2 virus vector showed Mycobacteria-specific immune responses by intranasal immunization. Vaccine 2014 32: 1727–1735. [PubMed: 24486310]
40. Matsuo K, Yamaguchi R, Yamazaki A, Tasaka H and Yamada T, Cloning and expression of the Mycobacterium bovis BCG gene for extracellular alpha antigen. J Bacteriol 1988 170: 3847–3854. [PubMed: 2842287]
41. Matsuo K, Yamaguchi R, Yamazaki A, Tasaka H, Terasaka K and Yamada T, Cloning and expression of the gene for the cross-reactive alpha antigen of Mycobacterium kansasii. Infect Immun 1990 58: 550–556. [PubMed: 2404875]
42. Yanagisawa S, Koike M, Kariyone A, Nagai S and Takatsu K, Mapping of V beta 11+ helper T cell epitopes on mycobacterial antigen in mouse primed with Mycobacterium tuberculosis. Int Immunol 1997 9: 227–237. [PubMed: 9040005]
43. Kariyone A, Higuchi K, Yamamoto S, Nagasaka-Kametaka A, Harada M, Takahashi A, Harada N, Ogasawara K and Takatsu K, Identification of amino acid residues of the T-cell epitope of Mycobacterium tuberculosis alpha antigen critical for Vbeta11(+) Th1 cells. Infect Immun 1999 67: 4312–4319. [PubMed: 10456868]
44. D'Souza S, Rosseels V, Romano M, Tanghe A, Denis O, Jurion F, Castiglione N, Vanonckelen A, Palfliet K and Huygen K, Mapping of murine Th1 helper T-Cell epitopes of mycolyl transferases Ag85A, Ag85B, and Ag85C from Mycobacterium tuberculosis. Infect Immun 2003 71: 483–493. [PubMed: 12496199]
45. Woodworth JS, Wu Y and Behar SM, Mycobacterium tuberculosis-specific CD8+ T cells require perforin to kill target cells and provide protection in vivo. J Immunol 2008 181: 8595–8603. [PubMed: 19050279]
46. Winau F, Weber S, Sad S, de Diego J, Hoops SL, Breiden B, Sandhoff K, Brinkmann V, Kaufmann SH and Schaible UE, Apoptotic vesicles crossprime CD8 T cells and protect against tuberculosis. Immunity 2006 24: 105–117. [PubMed: 16413927]
47. Woodworth JS and Behar SM, Mycobacterium tuberculosis-specific CD8+ T cells and their role in immunity. Crit Rev Immunol 2006 26: 317–352. [PubMed: 17073557]

48. Chen CY, Huang D, Wang RC, Shen L, Zeng G, Yao S, Shen Y, Halliday L, Fortman J, McAllister M, Estep J, Hunt R, Vasconcelos D, Du G, Porcelli SA, Larsen MH, Jacobs WR Jr., Haynes BF, Letvin NL and Chen ZW, A critical role for CD8 T cells in a nonhuman primate model of tuberculosis. PLoS Pathog 2009 5: e1000392.

49. Kaufmann SH, Tuberculosis vaccines: time to think about the next generation. Semin Immunol 2013 25: 172–181. [PubMed: 23706597]

50. McShane H, Jacobs WR, Fine PE, Reed SG, McMurray DN, Behr M, Williams A and Orme IM, BCG: myths, realities, and the need for alternative vaccine strategies. Tuberculosis (Edinb) 2012 92: 283–288. [PubMed: 22349516]

51. Orme IM, The use of animal models to guide rational vaccine design. Microbes Infect 2005 7: 905–910. [PubMed: 15878834]

52. Honda M, Wang R, Kong WP, Kanekiyo M, Akahata W, Xu L, Matsuo K, Natarajan K, Robinson H, Asher TE, Price DA, Douek DC, Margulies DH and Nabel GJ, Different vaccine vectors delivering the same antigen elicit CD8+ T cell responses with distinct clonotype and epitope specificity. J Immunol 2009 183: 2425–2434. [PubMed: 19620307]

53. Huygen K, The Immunodominant T-Cell Epitopes of the Mycolyl-Transferases of the Antigen 85 Complex of M. tuberculosis. Front Immunol 2014 5: 321. [PubMed: 25071781]

54. Content J, de la Cuvellerie A, De Wit L, Vincent-Levy-Frebault V, Ooms J and De Bruyn J, The genes coding for the antigen 85 complexes of Mycobacterium tuberculosis and Mycobacterium bovis BCG are members of a gene family: cloning, sequence determination, and genomic organization of the gene coding for antigen 85-C of M. tuberculosis. Infect Immun 1991 59: 3205–3212. [PubMed: 1715324]

55. Denis O, Tanghe A, Palfliet K, Jurion F, van den Berg TP, Vanonckelen A, Ooms J, Saman E, Ulmer JB, Content J and Huygen K, Vaccination with plasmid DNA encoding mycobacterial antigen 85A stimulates a CD4+ and CD8+ T-cell epitopic repertoire broader than that stimulated by Mycobacterium tuberculosis H37Rv infection. Infect Immun 1998 66: 1527–1533. [PubMed: 9529077]

56. Majlessi L, Rojas MJ, Brodin P and Leclerc C, CD8+-T-cell responses of Mycobacterium-infected mice to a newly identified major histocompatibility complex class I-restricted epitope shared by proteins of the ESAT-6 family. Infect Immun 2003 71: 7173–7177. [PubMed: 14638811]

57. Mitaksov V and Fremont DH, Structural definition of the H-2Kd peptide-binding motif. J Biol Chem 2006 281: 10618–10625. [PubMed: 16473882]

58. Samanta D, Mukherjee G, Ramagopal UA, Chaparro RJ, Nathenson SG, DiLorenzo TP and Almo SC, Structural and functional characterization of a single-chain peptide-MHC molecule that modulates both naive and activated CD8+ T cells. Proc Natl Acad Sci U S A 2011 108: 13682–13687. [PubMed: 21825122]

59. Zhou M, Xu Y, Lou Z, Cole DK, Li X, Liu Y, Tien P, Rao Z and Gao GF, Complex assembly, crystallization and preliminary X-ray crystallographic studies of MHC H-2Kd complexed with an HBV-core nonapeptide. Acta Crystallogr D Biol Crystallogr 2004 60: 1473–1475. [PubMed: 15272181]

60. Motozono C, Pearson JA, De Leenheer E, Rizkallah PJ, Beck K, Trimby A, Sewell AK, Wong FS and Cole DK, Distortion of the Major Histocompatibility Complex Class I Binding Groove to Accommodate an Insulin-derived 10-Mer Peptide. J Biol Chem 2015 290: 18924–18933. [PubMed: 26085090]

61. Liu WJ, Lan J, Liu K, Deng Y, Yao Y, Wu S, Chen H, Bao L, Zhang H, Zhao M, Wang Q, Han L, Chai Y, Qi J, Zhao J, Meng S, Qin C, Gao GF and Tan W, Protective T Cell Responses Featured by Concordant Recognition of Middle East Respiratory Syndrome Coronavirus-Derived CD8+ T Cell Epitopes and Host MHC. J Immunol 2017 198: 873–882. [PubMed: 27903740]

62. Matsuo K, Yamaguchi R, Yamazaki A, Tasaka H, Terasaka K, Totsuka M, Kobayashi K, Yukitake H and Yamada T, Establishment of a foreign antigen secretion system in mycobacteria. Infect Immun 1990 58: 4049–4054. [PubMed: 1701418]

63. Perfetto SP, Chattopadhyay PK and Roederer M, Seventeen-colour flow cytometry: unravelling the immune system. Nat Rev Immunol 2004 4: 648–655. [PubMed: 15286731]

64. Betts MR, Brenchley JM, Price DA, De Rosa SC, Douek DC, Roederer M and Koup RA, Sensitive and viable identification of antigen-specific CD8+ T cells by a flow cytometric assay for degranulation. J Immunol Methods 2003 281: 65–78. [PubMed: 14580882]

65. Cossarizza A, Chang HD, Radbruch A, Andrä I, Annunziato F, Bacher P, Barnaba V et al., Guidelines for the use of flow cytometry and cell sorting in immunological studies Eur. J. Immunol. 2017 47: 1584–1797.

66. Karlhofer FM, Ribaudo RK and Yokoyama WM, MHC class I alloantigen specificity of Ly-49+ IL-2-activated natural killer cells. Nature 1992 358: 66–70. [PubMed: 1614533]

67. Evans GA, Margulies DH, Shykind B, Seidman JG and Ozato K, Exon shuffling: mapping polymorphic determinants on hybrid mouse transplantation antigens. Nature 1982 300: 755–757. [PubMed: 6184620]

68. Tormo J, Natarajan K, Margulies DH and Mariuzza RA, Crystal structure of a lectin-like natural killer cell receptor bound to its MHC class I ligand. Nature 1999 402: 623–631. [PubMed: 10604468]

69. Wang R, Natarajan K and Margulies DH, Structural basis of the CD8 alpha beta/MHC class I interaction: focused recognition orients CD8 beta to a T cell proximal position. J Immunol 2009 183: 2554–2564. [PubMed: 19625641]

70. Kabsch W, Xds. Acta Crystallogr D Biol Crystallogr 2010 66: 125–132. [PubMed: 20124692]

71. McCoy AJ, Grosse-Kunstleve RW, Adams PD, Winn MD, Storoni LC and Read RJ, Phaser crystallographic software. J Appl Crystallogr 2007 40: 658–674. [PubMed: 19461840]

72. Adams PD, Grosse-Kunstleve RW, Hung LW, Ioerger TR, McCoy AJ, Moriarty NW, Read RJ, Sacchettini JC, Sauter NK and Terwilliger TC, PHENIX: building new software for automated crystallographic structure determination. Acta Crystallogr D Biol Crystallogr 2002 58: 1948–1954. [PubMed: 12393927]

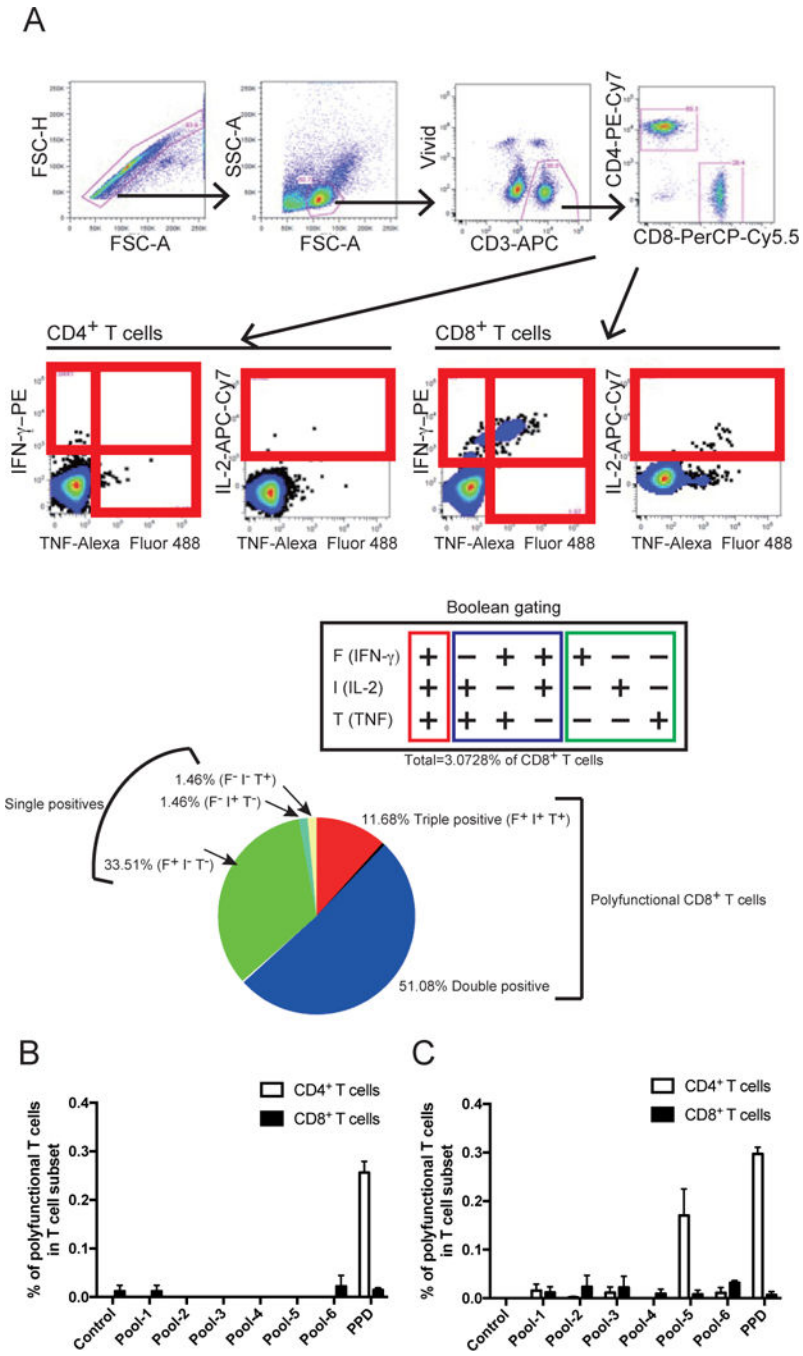

Figure 1. BCG vaccination does not induce polyfunctional CD8$^+$ T cells specific for major secretory protein *Mtb*85B.

(A) Gating tree for functional characterization of distinct populations of CD8$^+$ T cell responses using polychromatic flow cytometry. Shown is the gating strategy used to identify IFN-γ-, IL-2- and TNF-producing CD8$^+$ and CD4$^+$ T cells in splenocytes from a representative mouse immunized with rBCG-Mkan85B/DNA-Mkan85B. Upper 4 panels show initial gating of total events including a singlet cell gate; followed by selection for lymphocytes, live cells (ViViD$^-$) and live CD3$^+$ T cells were identified by ViViD$^-$CD3$^+$ cells. CD8$^+$ and CD4$^+$ T cells were further identified by CD8 and CD4 expression. Peptide-

specific IFN-γ-, IL-2- and TNF-producing $CD4^+$ T cells or $CD8^+$ T cells were gated as shown. The cells producing three, any two and any one cytokine were determined by Boolean combinations. Each cytokine-positive cell is assigned to one of seven possible combinations of these three cytokines ($F^+I^+T^+$, $F^-I^+T^+$, $F^+I^-T^+$, $F^+I^+T^-$, $F^+I^-T^-$, $F^-I^+T^-$ or $F^-I^-T^+$) and total of the cytokine producing cells were calculated as percent positives in $CD8^+$ T cells. The fraction of the total response consisting of cells producing three (3+), any two (2+) or any one (1+) cytokine is represented by a pie chart and sum of the three and two were measured as polyfunctional $CD8^+$ T cells specific for the epitope peptide. (B and C) $H2^d$ BALB/c (B) or $H2^b$ C57BL/6 (C) mice were immunized with BCG as described in Materials and Methods, spleen cells were harvested and restimulated *in vitro* with: no peptide (Control); the indicated overlapping peptide pools of *Mtb*85B; or with PPD. Percent (%) of $CD4^+$ (open bar) or $CD8^+$ (closed bar) T cells that produced multiple cytokines were counted as “polyfunctional” as described in detail in Materials and Methods. Data represent three independent experiments with five mice per group. Error bars represent SEM.

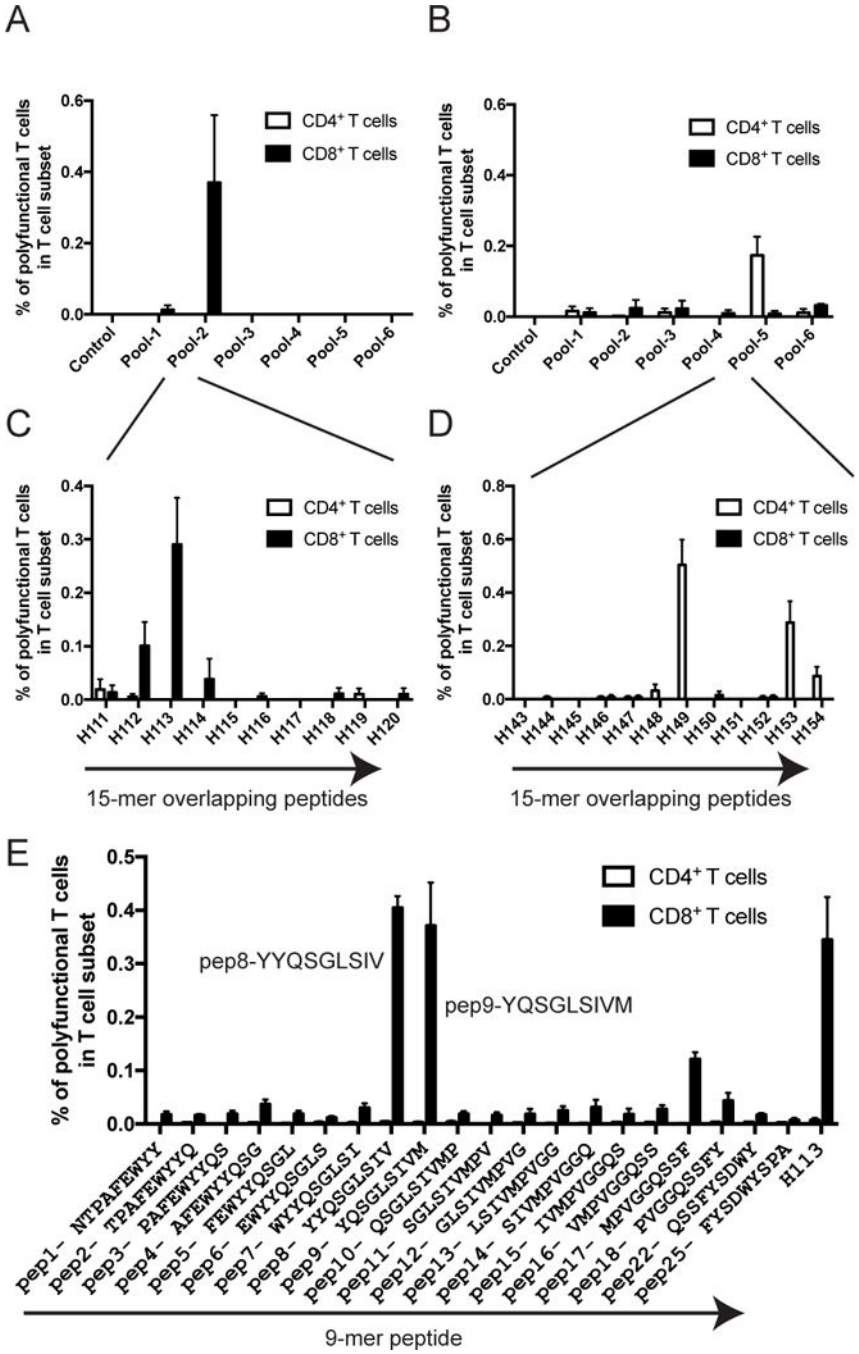

Figure 2. Screening of cross-reactive CD8$^+$ T cell epitopes of *Mtb* by *Mtb*85B peptides.

Induction of *Mtb*85B-specific polyfunctional CD8$^+$ and CD4$^+$ T cells by immunization consisting of priming with the rBCG-Mkan85B and boosting with DNA-Mkan85B three times in BALB/c (A) or C57BL/6 mice (B). Spleen cells were incubated with pooled (A, B) and individual (C, D) 15-mer overlapping peptides of *Mtb*85B for induction of polyfunctional CD8$^+$ and CD4$^+$ T cells as described in Materials and Methods. (E) Epitope mapping of *Mtb*85B peptide for induction of polyfunctional CD8$^+$ T cells stimulated with 9-mer peptide in BALB/c mice immunized with rBCG-Mkan85B followed by DNA-Mkan85B

boost. Polyfunctional epitope-sequences were termed as pep8 peptide with YYQSGLSIV and pep9 peptide with YQSGLSIVM sequences. H113 is a screened 15-mer peptide which contains both the pep8 and pep9 epitope sequences. Data represent three to five independent experiments with five mice per group. Error bars represent SEM.

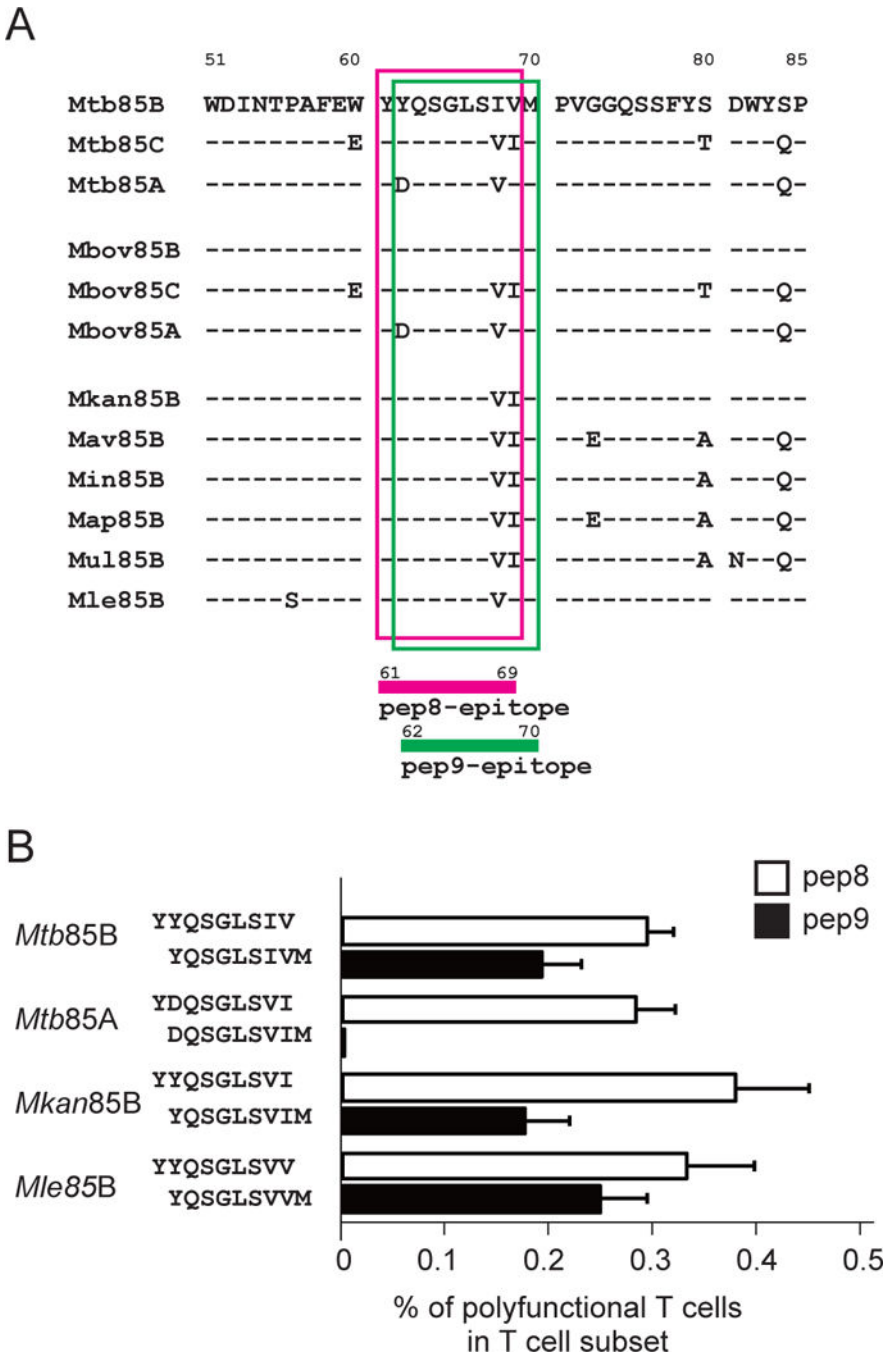

Figure 3. Differential stimulation of CD8$^+$ T cells with distinct specificity of the functional peptides.

(A) Alignment of the epitope pep8 and pep9 for polyfunctional CD8$^+$ T cell-induction on mycobacterium Ag85B complex. Amino acid sequence alignment of *Mtb* Ag85B (*Mtb*85B), *Mtb* Ag85C (*Mtb*85C), *Mtb* Ag85A (*Mtb*85A), *M. bovis* Ag85B (*Mbov*85B), *M. bovis* Ag85C (*Mbov*85C), *M. bovis* Ag85A (*Mbov*85A), *M. kansasii* Ag85B (*Mkan*85B), *M. avium* Ag85B (*Mav*85B), *M. intracellulaire* Ag85B (*Min*85B), *M. avium subsp. paratuberculosis* Ag85B (*Map*85B), *M. ulcerans* Ag85B (*Mul*85B) and *M. leprae* Ag85B (*Mle*85B). Amino acid sequence of *Mtb*85B and its differences from other *mycobacterium*

sequences are shown in single letter code. pep8 and pep9 epitopes of *mycobacterium* Ag85B complex are highlighted with magenta and green line-rectangles, respectively. (B) Cross-reactivity and functionality between pep8 and pep9 for the induction of polyfunctional $CD8^+$ T cells in immunized animals. The second position of the aspartic acid (D) at amino acid 62 in antigen 85A complex is critical for activation of $CD8^+$ T cells in $H2^d$ mice, whereas those of the tyrosine (Y) at amino acid 62 in Ag85B complexes of *Mtb*85B, *Mkan*85B and *Mle*85B are cross-reactive. Substitutions of the eighth and ninth positions of valine (V) isoleucine (I) with either VI, IV and VV functions as epitope peptides. Data represent three independent experiments with five mice per group. Error bars represent SEM.

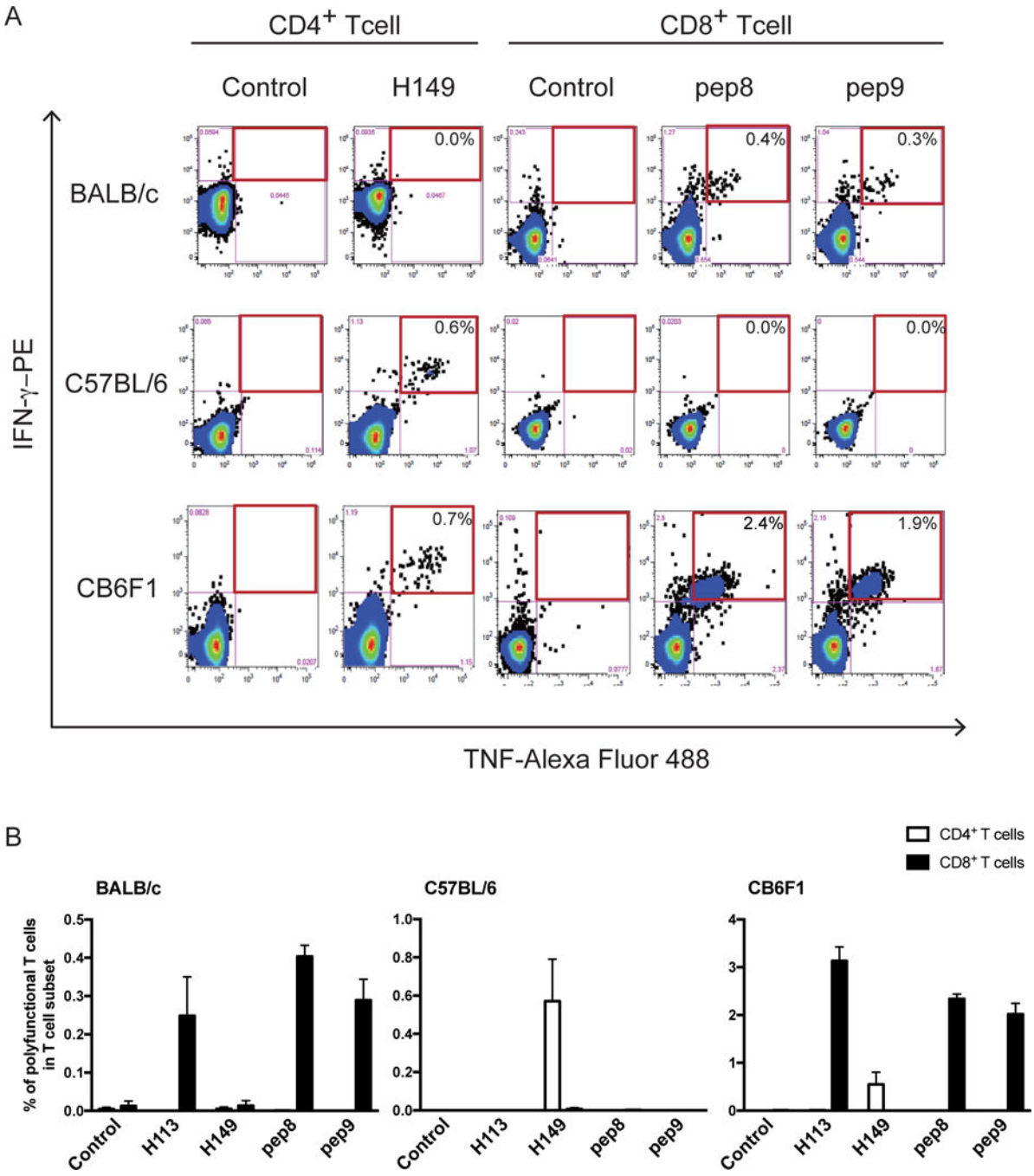

Figure 4. Augmented induction of *Mtb*85B-specific polyfunctional CD8$^+$ T cells by co-inducing CD4$^+$ T cells in CB6F1 mice.

(A) Representative fluorogram of epitope-specific polyfunctional CD8$^+$ and CD4$^+$ T cell-inductions in splenocytes from C57BL/6, BALB/c and CB6F1 mice, with TNF-Alexa Fluor 488 on x-axis and IFN-**γ**-PE on y-axis. (B) Augmented induction of the polyfunctional CD8$^+$ T cells in H2$^{b/d}$ CB6F1 mice. Polyfunctional CD8$^+$ T cell induction by stimulation with 9-mer-peptides in BALB/c mice immunized with the regimen (left panel). C57BL/6 mice immunized with the prime boost regimen induce polyfunctional CD4$^+$ T cells by stimulation with 15-mer-peptides (middle panel). The polyfunctional CD8$^+$ T cell inductions

were augmented by co-inducing the polyfunctional $CD4^+$ T cells in the CB6F1 mice by rBCG-Mkan85B priming followed by boosting with DNA-Mkan85B three times (right panel). Data represent three independent experiments with five mice per group. Error bars represent SEM.

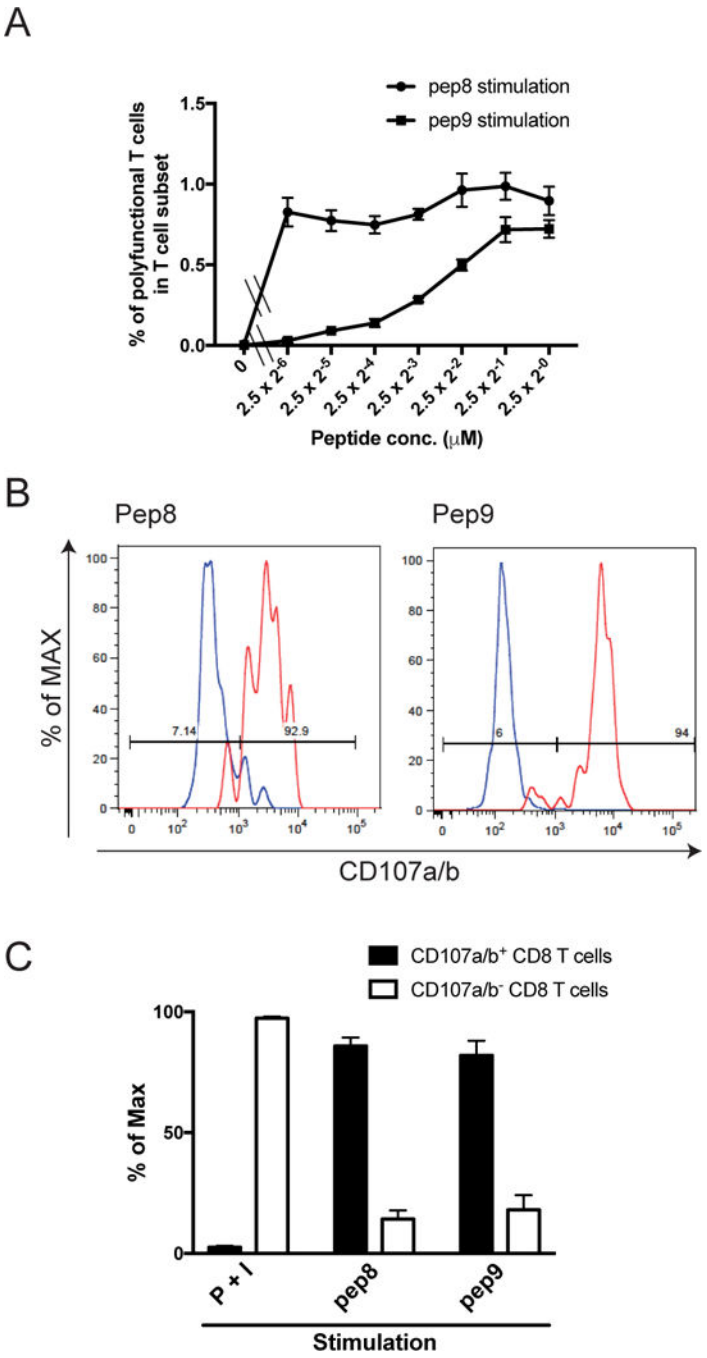

Figure 5. Functional properties of the epitope specific polyfunctional CD8$^+$ T cells.

BALB/c mice were immunized with rBCG-Mkan85B followed by boosting with DNA-Mkan85B three times. Spleen cells from the immunized mice were stimulated with pep8 and pep9 peptide. (A) Different dose-response-generation of polyfunctional CD8$^+$ T cells by the epitope peptides. pep8 is much more functional for the CD8$^+$ T cell induction than pep9 stimulation of immune T cells by comparing the 50% stimulation dose between the functional pep8 and pep9. Data represent three independent experiments with three mice per group. Error bars represents SEM. (B) Representative histograms of CD107a/b expression.

The polyfunctional and effector cytokines-producing $CD8^+$ T cells were analyzed for expression of CD107a/b. Percentages of maximal expression with CD107a/b (% of max) are presented in histograms of red line (polyfunctional $CD8^+$ T cells of pep8 or pep9-stimulations, left and right panels, respectively) and of blue line (polyfunctional) $CD8^+$ T cells of simultaneous stimulation with PMA and ionomycin (P+I)), which were mainly negative of CD107a/b expression. (C) Expression of CD107a/b on the polyfunctional $CD8^+$ T cells. Data are presented as the percentage of the CD107a/b expression in the polyfunctional cells (closed bar), and CD107a/b negatively (open bar) in the P+I, pep8 or pep9 -stimulated polyfunctional $CD8^+$ T cells. Data represent three independent experiments with five mice per group. Error bars represent SEM.

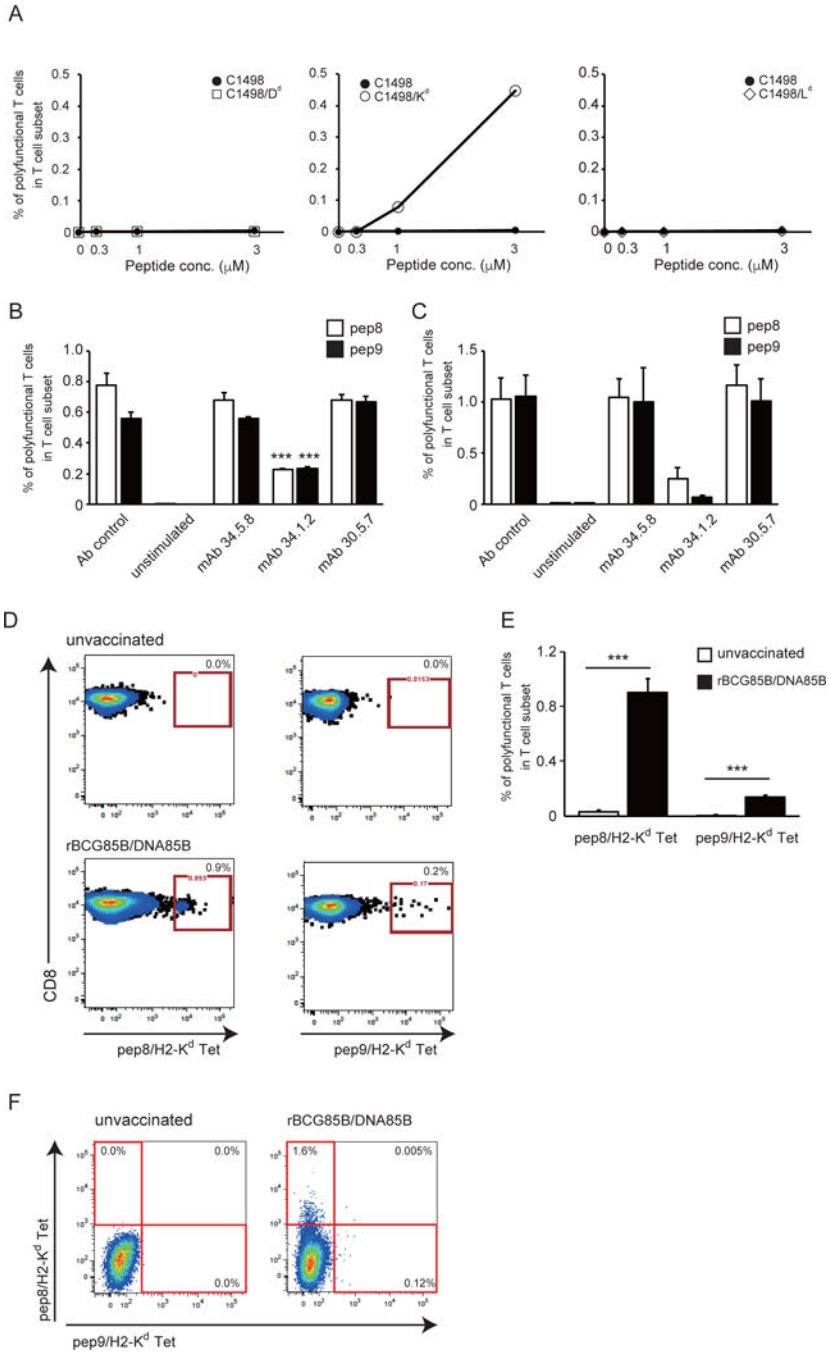

Figure 6. H2-K^d alloantigen specificity for induction of the epitope peptide-stimulated polyfunctional T cells.

(A) C1498 cells transfected with H2-D^d, H2-K^d or H2-L^d were incubated with pep9 peptide and used as stimulator cells for polyfunctional T cell induction with various ratio of effector and stimulator cells; 0, 0.3, 1 and 3. Splenocytes from BALB/c mice immunized with rBCG-Mkan85B/DNA-Mkan85B were incubated in the presence of medium alone or the stimulator cells for 6 h and the polyfunctional T cell induction was analyzed by flow cytometry. (B and C) MHC-I alloantigen specificity of pep8 and pep9. Spleen cells from rBCG-Mkan85B/DNA-Mkan85B immunized BALB/c (B) and CB6F1 (C) mice were

incubated with mAb 34.5.8 (anti-H-2D^d antibody), mAb 34.1.2 (anti-H2-K^{d}D^d antibody) or mAb 30.5.7 (anti-H2-L^d antibody), followed by stimulation with the pep8 or pep9 for polyfunctional T cell assays. (D) Representative fluorogram of reactivity of pep8/H-2K^d and pep9/H-2K^d tetramer-positive CD8$^+$ T cells from rBCG-Mkan85B/DNA-Mkan85B immunized BALB/c mice, with pep8/H-2K^d (left panel) or pep9/H-2K^d (right panel) on x-axis and CD8 on y-axis. Control refers to immunization with vector alone. Spleen cells from BALB/c mice were analyzed for reactivity with the pep8/H-2K^d tetramer conjugated to allophycocyanin (APC) or with the pep9 /H-2K^d tetramer conjugated to phycoerythrin (PE). (E) pep8/H-2K^d and pep9 /H-2K^d tetramer-positive CD8$^+$ cell responses in the mice immunized with rBCG-Mkan85B/DNA-Mkan85B (closed bar) or control (open bar). Data represent three independent experiments with five mice per group. ***, $p < 0.001$; one-way ANOVA test. Error bars represent SEM. (F) Representative fluorogram of double staining with the two tetramers labelled with different fluorochromes with pep9/H-2K^d on x-axis and pep8/H-2K^d on y-axis. Percentage of positive cells is indicated in each quadrant.

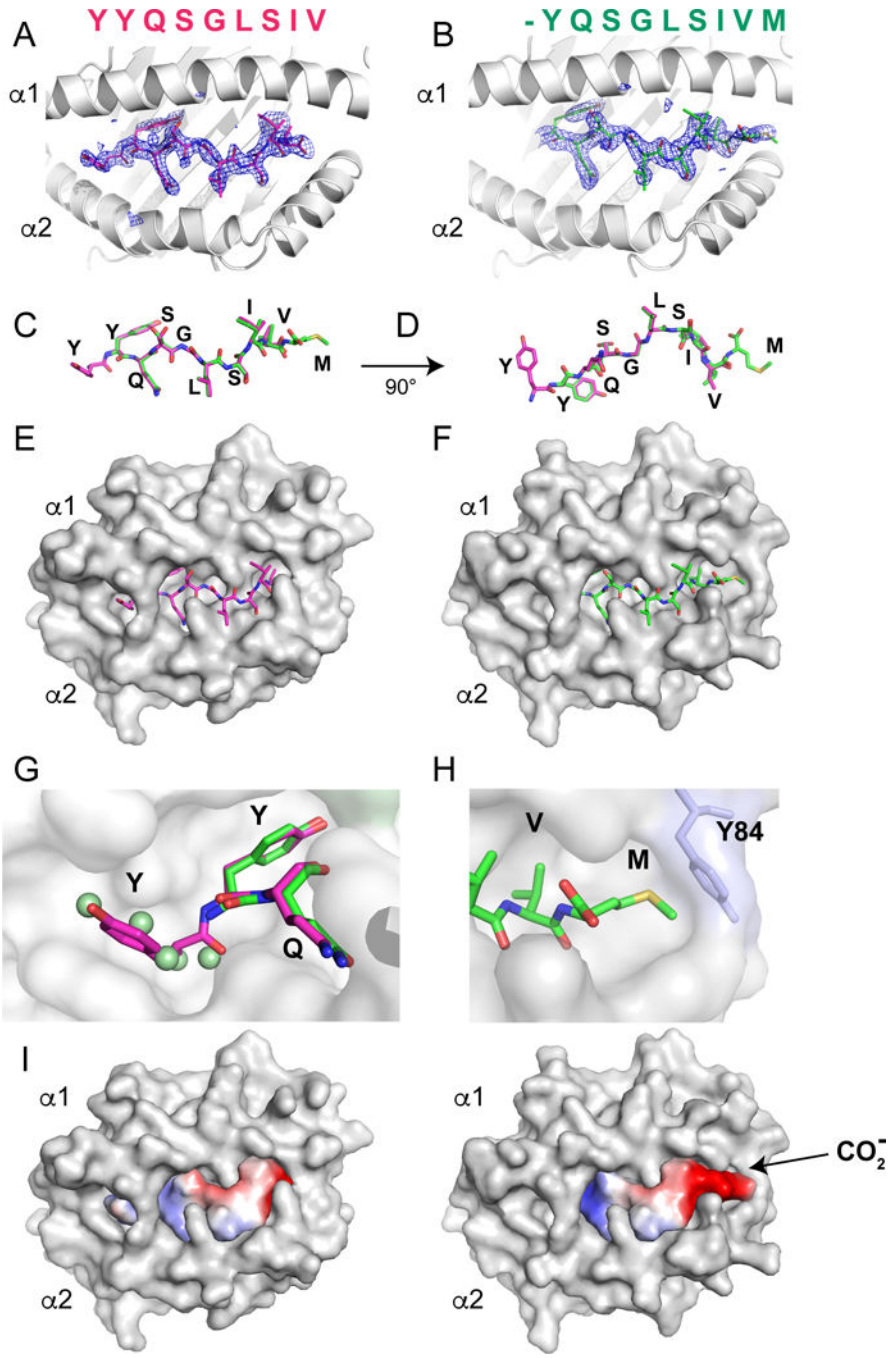

Figure 7. Structures of peptide/H2-K^d complexes reveal different frames of pep8 and pep9 interaction in peptide binding groove.

Graphics illustration of pep8 (A. C, E, G) and pep9 (B, D, F, H) complexed with H2-K^d depicted as ribbon cartoon (A, B), bare stick of peptide (C, D), or with H2-K^d in surface representation (E, F). Omit maps, calculated without peptide model, are shown with superposed stick model for pep8 (A, magenta) or pep9 (B, green). Superposition of pep8 and pep9 (C, D) emphasizes similarity of peptide backbone. (G) Close-up of region of pockets A and B shows how pep8 pY1 (magenta) sits in pocket A, and both pep8 pY2 and pep9 pY1 sit in pocket B. Note that five water molecules (green spheres) occupy pocket A in the pep9

structure. To allow visualization of the A and B pockets, the surface representation of the salt bridge H2-K^{d}R66 to E163 has been removed. (H) Close-up of C-terminal residues pV8 and pM9 illustrates pV8 anchored in pocket F, p9M laying flat in an additional concavity. Note that the terminal carboxylate is flipped for surface exposure by this configuration (G, H). (I) Surface charge distribution (calculated with PyMOL) of peptides pep8 and pep9 is shown (acidic, red; basic, blue).

Table 1

X-ray data collection and refinement statistics

	pep8/H2-K^d/hβ_2m	pep9/H2-K^d/hβ_2m
PEPTIDE	**YYQSGLSIV**	**YQSGLSIVM**
PDB ID	**5TS1**	**5TRZ**
Data collection		
Space group	P1	$P2_1$
Cell dimensions		
a, *b*, *c* (Å)	47.30, 88.96, 109.95	46.63, 88.82, 110.75
α, *β*, *γ* (°)	89.97, 93.83, 90.04	90.00, 89.99, 90.00
Resolution (Å)	47–2.30 (2.38–2.30) *	55–2.25 (2.33–2.25)
R_{sym} or R_{merge} (%)	23.2 (118.2)	8.4 (49.8)
$I/\sigma I$	6.9 (1.3)	19.4 (4.6)
Completeness (%)	98.2 (97.4)	95.3 (57.1)
Redundancy	3.9 (4.0)	7.4 (6.9)
R_{pim} (%)	13.5 (68.8)	3.3 (20.2)
CC½ (%)	97.9 (48.8)	99.9 (94.7)
Twin fraction	0.450 (-h,k,-l)	0.478 (h,-k,-l)
Refinement		
Resolution (Å)	47–2.30 (2.38–2.30)	55–2.25 (2.33–2.25)
No. reflections (unique)	78045	41172
R_{work}/R_{free} (%)	18.7(23.9)/22.5(30.8)	17.1(22.9)/19.8(29.2)
No. atoms	13146	6619
H2-K^d/hβ_2m	12334	6155
Peptide	292	138
B-factors (Å^2) (Wilson/Average)	23.8/26.0	28.0/38.0
H2-K^d/hβ_2m	26.5	38.9
Peptide	20.3	33.6
R.m.s deviation		
Bond lengths (Å)	0.007	0.004
Bond angles (°)	1.20	0.80
Ramachandran favored/outlier (%)	97.0/0.7	97.0/0.3

* Highest resolution shell is shown in parenthesis.